International Journal of Geophysics and Geochemistry
2018; 5(1): 19-26
http://www.aascit.org/journal/ijgg
ISSN: 2381-1099 (Print); ISSN: 2381-1102 (Online)

American Association for Science and Technology

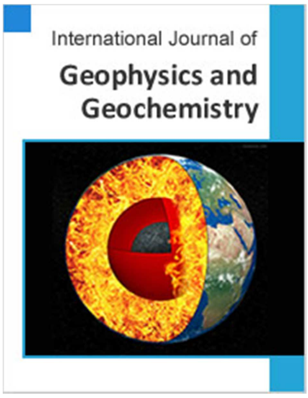

Keywords
Thermal Perturbations,
Seepage of Meteoric Waters,
Climate History,
Semiarid Regions,
Electrical Resistivity Profile

Received: January 22, 2018
Accepted: February 6, 2018
Published: March 2, 2018

Subsurface Thermal Perturbations by Seepage of Meteoric Waters

Jorge Luiz dos Santos Gomes[1, 2], **Fábio Pinto Vieira**[1], **Valiya Mannathal Hamza**[1, *]

[1]Department of Geophysics, Observatório Nacional, Rio de Janeiro, Brazil
[2]Institute of Science Engineering and Technology, Universidade Federal dos Vales do Jequitinhonha e Mucuri, Teófilo Otoni, Brazil

Email address
Jorge.gomes.br@gmail.com (J. L. dos S. Gomes), fabiovieira@on.br (F. P. Vieira), hamza@on.br (V. M. Hamza)
[*]Corresponding author

Citation
Jorge Luiz dos Santos Gomes, Fábio Pinto Vieira, Valiya Mannathal Hamza. Subsurface Thermal Perturbations by Seepage of Meteoric Waters. *International Journal of Geophysics and Geochemistry.* Vol. 5, No. 1, 2018, pp. 19-26.

Abstract
The focus of the present work is on investigating the nature of thermal anomalies at shallow depths generated by seepage of meteoric waters and its perturbing effects on the climate history deduced from analysis of borehole temperature logs. The study was carried out at a locality in the semiarid region of southeast Brazil. Results of electrical resistivity soundings were employed in mapping seepage zones. Analysis of temperature data from boreholes indicate that seepage of relatively cold meteoric waters leads to localized thermal anomalies at shallow depths. Consequently, seepage effects are found to be capable of leading to overestimation of changes in ground surface temperatures (GST) and underestimation of the age of climate warming episodes. However, seepage processes occur mainly in arid and semiarid regions and hence the proposed corrections are likely to be important in geothermal climate studies of sites in tropical and subtropical latitudes. Results of model studies are presented illustrating how effects of perturbations by seepage can be evaluated. It is proposed that use of geothermal methods for estimation of GST changes, based on analysis of temperature log data of boreholes in semiarid regions, should include evaluation of subsurface permeable zones.

1. Introduction

Analysis of subsurface temperature data have been carried out by many researchers in attempts to estimate past ground surface temperatures (e.g., [1, 2, 3, 4, 5] Most of the earlier works assumed conductive regime and these have shown to lead to somewhat equivalent results [2, 6, 7, 8]. Thus, inversion of borehole temperatures to obtain estimates of past ground surface temperatures (GST) has been widely employed as a convenient technique in assessment of climate changes of the recent past. Even though spatial variations in slope and elevation as well as spatial and temporal variations in land cover may contribute to changes in GST, the method is widely believed to provide both reliable long-term-average GST and its past variations at a particular site.

In geothermal climate change studies, it is usual practice to consider GST as the boundary condition at the top of the conductive underground regime, which may or may not coincide with the ground surface. It implies that GST histories inverted from borehole temperature data are site specific. Nevertheless, recent results [9, 10] point to significant coupling between thermal fields and hydrologic processes interacting with the soil cover. In particular, there are clear indications that seepage of meteoric waters, with temperatures different from that soil layers, leads to alterations in the thermal regime of near-surface layers. In understanding true GST history these effects must be modeled and accounted for.

Nevertheless, few efforts have been made so far in studies of geothermal climate change, for evaluating thermal perturbations of soil layers induced by seepage of relatively cold waters of meteoric origin. Seepage flows, derived from rainwaters with significantly lower temperatures, are colder than soil layers at the ground surface. It is clear that seepage of cold meteoric waters could lead to subsurface thermal perturbations, which are not directly related to changes in GST originating from recent climate changes. However, seepage processes occur mainly in arid and semiarid regions and hence the proposed corrections are likely to be important in geothermal climate studies of tropical and subtropical latitudes. The objective of the present work is in analysis of climate signals extracted from borehole temperature data, at a site in Brazil where geoelectric methods have been employed for mapping seepage zones.

2. Characteristics of the Study Area

The study area is located in the municipality of Jenipapo de Minas, in southeast Brazil. According to results of geological studies, the rock formations in this region are composed predominantly by the Salinas formation (pEms) of the Macaúbas Group. In the east, according to [11] there are areas of Quaternary sedimentary rocks (QTd). These are composed of alluvium - colluvium deposits, overlying tertiary plateau surfaces. Geologic mapping has also identified occurrences of Tertiary sediments of the São Domingos Formation (Tsd). The outlines of local geologic units of the study area are illustrated in the map of Figure 1. This map also provides an overview of the drainage system in the study area. The green colored curve in the map of Figure 1 indicates the Setubal River, which is perennial. The red colored curve indicates the local stream Bolas, which is intermittent, having no surface runoff (water flow) during the dry season.

The hydrogeological domains in the municipality of Jenipapo de Minas are determined by two dominant rock types: 1) Neoproterozoic metamorphic rocks and Paleozoic granites, which constitute highly fractured rock formations, but which are relatively impermeable; 2) Cenozoic detrital covers, which are highly permeable for groundwater flows. As a result, the aquifers in these domains can be considered as falling into categories of near impermeable fractured systems and highly permeable granular systems. The hydrogeological potential of the fissure system is dependent on the intercommunication of the discontinuities, an aspect that usually translates to random and small-scale reservoirs [12]. It occurs throughout the municipality and is related to the rock types of the Macaúbas Group and the Mangabeiras granite. In general, it presents low hydrogeological potential, with structural features responsible for local variations in groundwater productivity. The granular aquifer system is represented by poorly consolidated sediments, which constitute the detrital deposits of sand-clay composition.

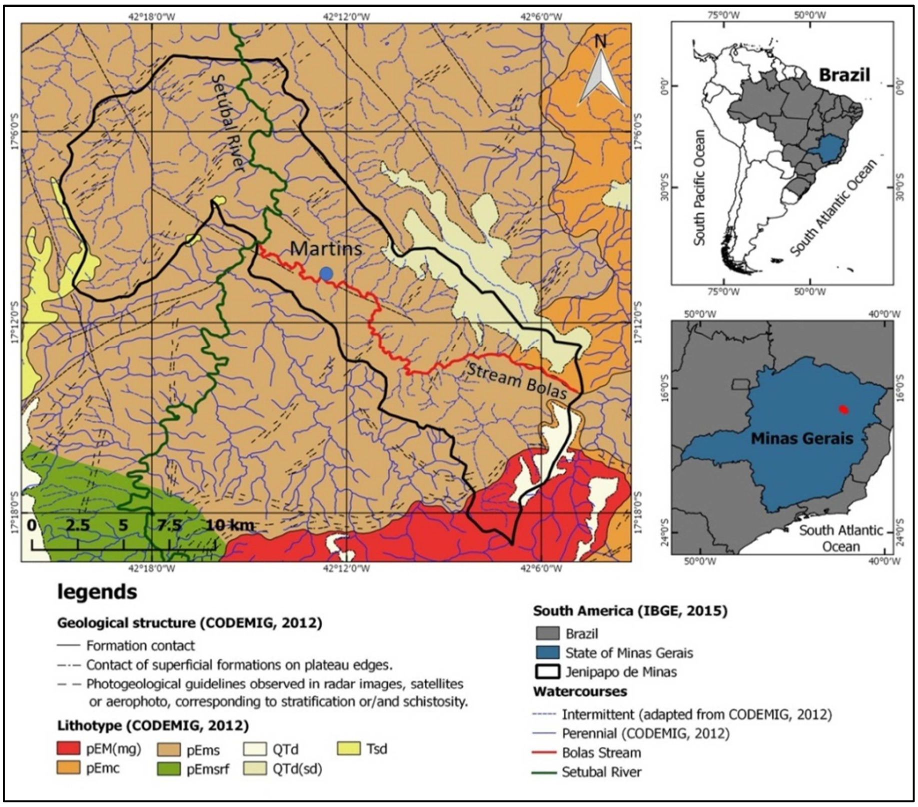

Figure 1. *Map of selected geological features and drainage systems in the study area. The blue circle indicates the locality where geophysical studies were carried out. Adapted with modifications from [11, 12].*

3. Electrical Resistivity Soundings

The objective of geoelectric studies has been to map subsurface structures associated with seepage of meteoric waters at shallow depths in the study area. The justification for the methodology adopted is that in regions of near uniform lithology relative changes in electrical resistivity may be considered as indicative of seepage zones of meteoric waters. The locality Martins, indicated in the map of Figure 1 refer to the site where geoelectric soundings were carried out. This is also the site where a borehole has been drilled in the year 2005, as part of local groundwater exploration. Examination of drill cuttings from this well indicates that rock formations at shallow depths are laterite deposits with good porosity and permeability [10, 12].

A detailed electrical resistivity survey was carried out during the end of the rainy season in April of 2017. At this time, there were occasional episodes of localized precipitation. But it did not lead to fluvial discharges during the survey period. AGI Super Sting resistivity equipment was used in data acquisition. Dipole-dipole arrangement was adopted for electrode configuration, with spacing of four meters. Measurements were carried out along a north-south profile, at the site indicated in Figure 2. The profile crosses the bed of the non-perennial stream Bolas and also its adjacent shoulders. This stream is intermittent and had no water flow at the time of survey.

The built-in software of the equipment allowed automatic acquisition and display of field data. The pseudo locations of the resistivity measurement data of geoelectric profiles in depth are composed of 7 layers (n) at depths of 1.67m (n1), 2.78m (n2), 3.84m (n3), 4.87m (n4), 5.57m (n5), 7.68m (n6) and 9.74m (n7). In this work, the term “pseudo location” was adopted for survey data, as the initial stages of data analysis did not consider the surface elevation, but only the array location. The surface elevations are considered in the second stage of data analysis when inversion schemes were employed in data analysis.

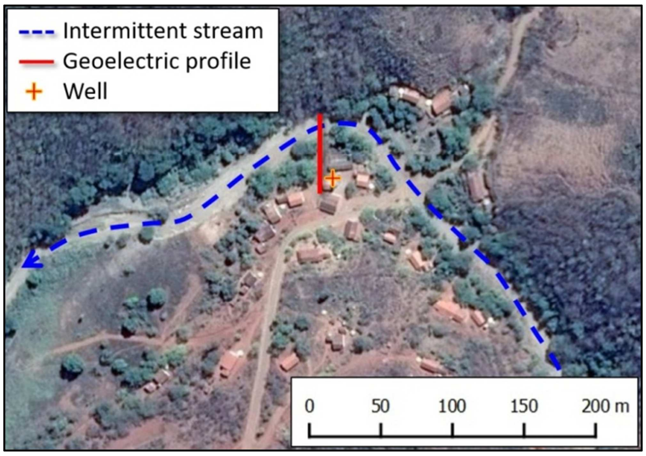

Figure 2. Locations of geoelectric profile (red line) and borehole (cross sign) at the site Martins. The blue dashed curve indicates the course of the intermittent stream Bolas.

During the initial phase, data acquired in the field were processed using the Earth Imager 2D software. Finite element techniques [13, 14, 15] were employed in data processing and in elaboration of electric resistivity model of the soil cover. The Cholesky decomposition technique was adopted in solving the model equations. The main purpose has been to reduce misfit between field measurements and calculated values of a physically plausible model. An inversion method, based on procedure proposed by [16] was employed in processing field data obtained in electrical resistivity surveys. One of the objectives of the inversion has been to find a resistivity model whose response (predicted values) best fits the measured data. The goodness of fit was characterized by calculating percent values of root mean square (RMS) error shown in the left panel of Figure 3. For purposes of qualitative evaluation of data analysis, a cross plot of the measured apparent resistivity data per predicted value was generated for the survey. The coherence between them is illustrated in the right panel of Figure 3.

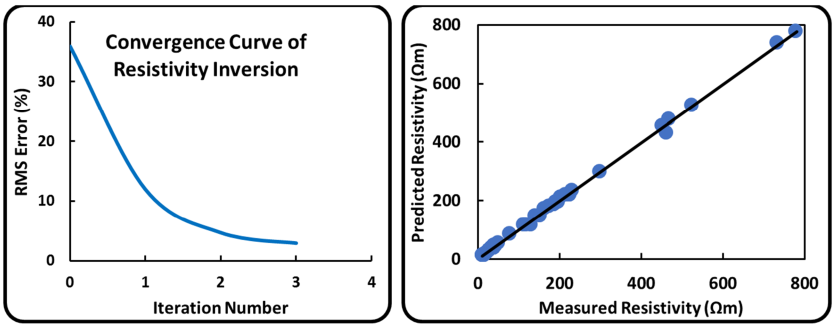

Figure 3. Illustrations of the results of inversion procedure. The left panel refer to variations in RMS error values as function of iteration number. The right panel is cross plot of measured and predicted apparent resistivity data.

The pseudo section of the geoelectric profile is illustrated in Figure 4. The black arrows in this Figure indicate approximate limits of the Bolas stream, whose margins are indicated by the abbreviations RM and LM. The orientation of the profile is along the north – south direction. In this section, the profile cut across the stream bed, which is devoid of vegetation cover and deposits by stream flow. A remarkable feature in Figure 4 is the presence of an upper layer of low resistivity (< 100Ωm) along the entire left margin of the profile, where soils rich in clay materials are present. This is in marked contrast with the resistivity values in excess of 500Ωm, found along the northern section.

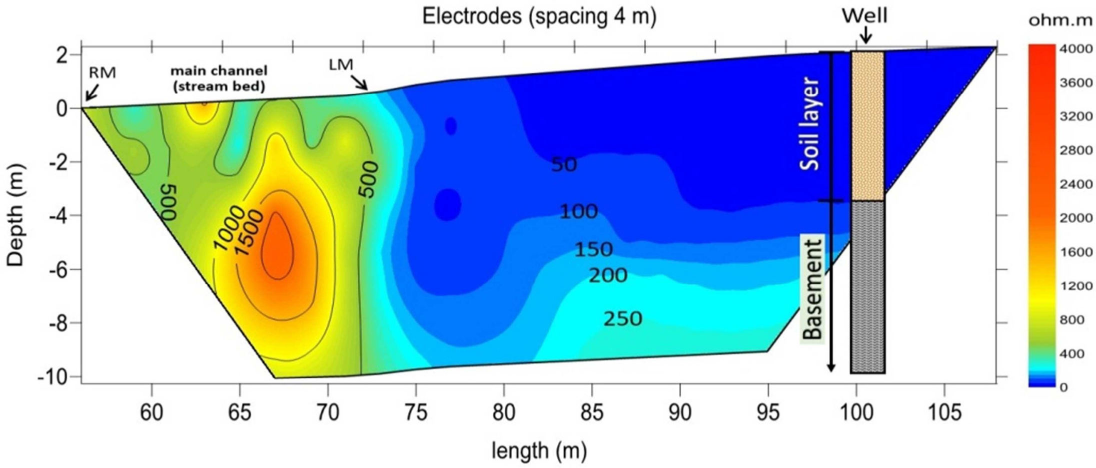

Figure 4. *The electrical resistivity profile across the study area, illustrating resistivity changes in near surface layers. The rectangular column on the right side refer to lithologic sequences encountered in the well drilled for groundwater.*

Identification of rock types responsible for the observed electrical resistivity contrast has also been made by examining the descriptive log of a water well drilled at the site. According to log data of this well, the top layer is sedimentary soil extend to a depth of 5.4m. The deeper parts of this well penetrate Precambrian schists, which extend to depths of at least 104m. Based on lithologic sequences identified in log data of this well it has been possible to establish an association of the upper zone in the left margin (LM) with water saturated layers beneath soil cover, where electrical resistivity values fall in the range of 7.5 to about 100Ωm. These evidences have been considered as indication that seepage of meteoric water is taking place along southern part of the profile.

4. Distribution of Subsurface Temperatures

Results of temperature log of the well at the locality of Martins provides information on the subsurface thermal field (see figure 5). The left panel of this figure reveals that subsurface layers at shallow depths are at temperatures lower than the mean annual surface temperatures. The vertical distribution is characterized by steadily decreasing values and are found to fall along a curve, with convexity towards the depth axis. Such curvatures in temperature logs are often considered as arising from increase in ground surface temperatures (GST), a consequence of recent warming of local climate. Under such conditions the thermal regime at shallow depths is transient in character. Its temporal evolution is determined to a large extent by the history of thermal energy exchange at the ground surface.

On the other hand, the dashed line in this figure indicates values of temperatures at depths less than 100 meters, inferred from results of temperature logs of deeper boreholes in nearby localities. It may be considered as representing the steady component of the temperature field, determined by the outflow of heat from the Earth's interior, free from effects of recent climate changes. It is clear that the observational data falling along the curve at depths less than 100 meters arise from superposition of steady and transient components of the temperature field at shallow depths.

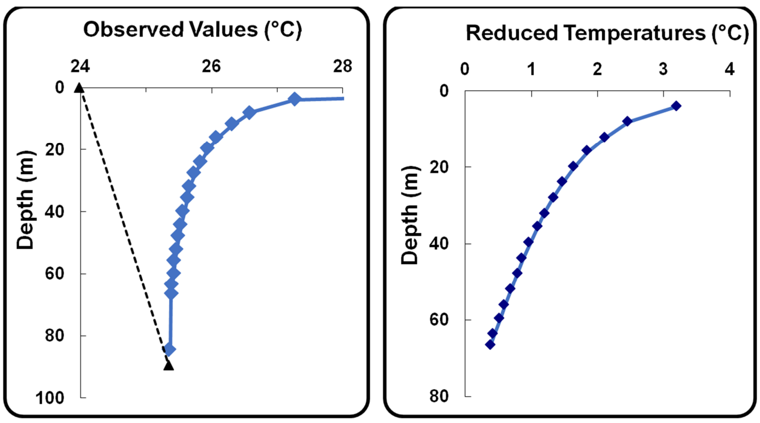

Figure 5. *Vertical distribution of temperatures in the well at Martins. The square symbols indicate observational data. The dashed line in the left panel indicates distribution of temperatures inferred from temperature logs of deep boreholes in nearby localities, considered as unaffected by recent climate changes. The right panel indicates the reduced temperatures.*

The basic steps in geothermal climate studies include identification and separation of the steady and transient components present in temperature profiles at shallow depths. Usually a linear fit to the deeper portion of log data from deeper boreholes, where climate perturbation is practically absent, allows determination of the local temperature gradient. Subtracting it from the observed temperatures allows determination of the transient component. Such values, often designated as "reduced temperatures", can now be considered in analysis of the climate signal. The vertical distribution of reduced temperatures for the well at Martins is illustrated in the right panel of Figure 5. Model studies of climate change may now be employed in analysis of reduced temperatures. In the present work, forward modelling approach has been adopted, the basic principles of which has been discussed extensively in the literature [1, 4, 5, 17, 18].

For cases where surface temperature variation can be represented by a power law relation, analytic solutions are readily available. Thus, for a linear (or ramp type) change in surface temperature the relation between the amplitude of the climate signal (ΔT) and the time elapsed (t) at any depth (z) is given by the relation [19]:

$$\Delta T\ (z) = 4\, \Delta T\ i^2\ erfc\ (z/\sqrt{4\alpha t}) \tag{1}$$

where i^2 *erfc* is the second integral of the complementary error function and α the thermal diffusivity of the medium. It may be written as:

$$T = T_m \left\{\left[1 + 2\left(\frac{z^2}{4\,\alpha\, t}\right)\right] erfc\left(\frac{z}{\sqrt{4\,\alpha\, t}}\right) - \frac{2}{\sqrt{\pi}}\left(\frac{z}{\sqrt{4\,\alpha\, t}}\right) \exp(-\frac{z^2}{4\,\alpha\, t})\right\} \tag{2}$$

In inversion procedures the best fitting ramp function is obtained by inverting the above relation using iterative procedures such as linearized Newton's method. The iterative procedure for this model, referred to as Ramp Inversion [20, 21, 22] allows simultaneous determination of the magnitude of surface temperature change and the period of its occurrence. Figure 6 below illustrates the model fit to reduced temperatures. Note that the observational data are bracketed by model fits for GST changes of 2.4 and 3.4°C occurring over the last 80 years.

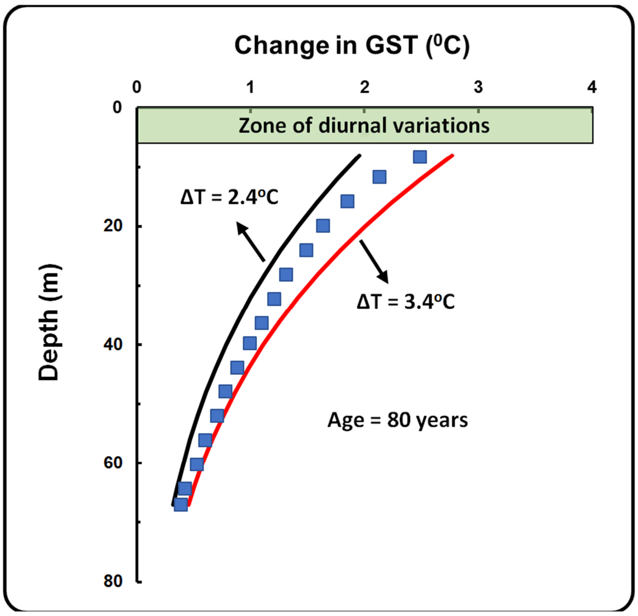

Figure 6. *Ramp function fits to reduced temperatures. Square symbols indicate observational data. Continuous lines are model fits based on equation -2. Black and red curves indicate respectively lower and upper limits for surface temperature changes (GST) of the recent past.*

4.1. Thermal Effects of Seepage

It is well known that meteoric waters in tropical and subtropical latitudes have temperatures lower than the ground surface temperatures. In such cases, downward seepage of meteoric waters induces cooling of subsoil layers. As a result, isotherms in the zone affected by seepage are pushed down to larger depth values. This has a marked effect on the curvatures of reduced temperatures profiles at shallow depths. In other words, thermal model fits based on such values, perturbed by seepage processes, can lead to substantial errors in determination of magnitudes and ages of climate signals.

A rigorous estimation of such temperature changes at shallow depths require knowledge of the temperature contrasts of meteoric waters, penetration depth of seepage, flow velocities in the soils and thermal properties of near surface layers. The model proposed by [23] is often employed in estimating temperature distributions in confined groundwater systems with vertical fluid fluxes. In such cases, the relation describing temperature distribution is:

$$\frac{T_Z - T_0}{T_L - T_0} = \left[\frac{\exp(\beta\ Z/L) - 1}{\exp(\beta) - 1}\right] \tag{3}$$

where T_L and T_0 are temperatures at the top and bottom boundaries respectively, L the thickness of the confined aquifer and β the Peclet number, which represents the ratio of thermal energy transported by advection to that by conduction. The relation for β is $\rho CvL/\lambda$, where λ is the thermal conductivity of the medium, ρC the thermal capacity, of the fluids in the pore space and v_z velocity components of fluids in the direction z. A problem with this model is the assumption that the velocity of fluid flow is constant throughout the aquitard.

In the present work, an alternative approach has been adopted which allows for the condition that seepage velocity is maximum at the top boundary, but it decreases rapidly with depth. The relation employed for determination of the depth changes arising from seepage flow is:

$$z_c = z_L\ [1 - \frac{\exp(z_L - z)}{z^* * z_L}] \tag{4}$$

where z_c is the depth change in temperature, z_L depth to bottom of the seepage zone and z^* a characteristic value for the depth factor of the seepage velocity. Note that z_c becomes zero at the bottom of the seepage zone ($z = z_L$).

Equation 4 leads to a set of depth values corresponding to the measured temperatures, the lower limit of which is anchored at depth z_L. This depth level, where seepage become insignificant, can be estimated from model fits to deeper parts of the curve of reduced temperatures. The depths corresponding to temperatures in the interval of *0* to z_L fall along a family of curves that depend on the value chosen for scale factor z^*. A suitable choice is the curve, the extrapolation of which to the depth level of zero coincides with the value of mean annual surface temperature. An example of the procedure outlined above is presented in Figure 7 for the log data of the well at Martins, where the values corrected for seepage effects are indicated by triangles. The model fits suggest a value of nearly 40 meters for z_L and a value of about *2* for the scale factor z^*. The corrected depth values in this figure are indicated by filled triangles. The dashed lines in black and red color refer to model curves that bracket the corrected depth values. The surface temperatures of these model curves are respectively 1.9 and 2.3°C. The square symbols, which indicate uncorrected depth values, are found to fall along a model curve for a surface temperature of 2.9°C.

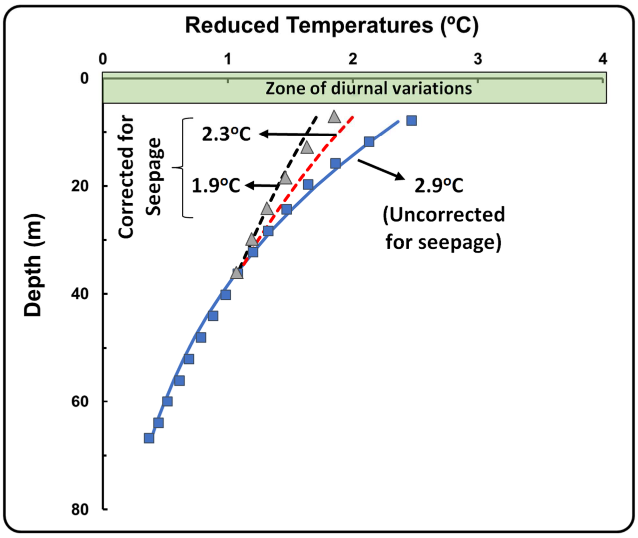

Figure 7. *Seepage model fits to reduced temperatures with corrected depth values. The square symbols indicate observational data. The triangles are data corrected for seepage effects. The continuous curve in blue color is the model fit, uncorrected for seepage effects. The dashed curves in green and red colors are model fits that incorporate seepage effects.*

4.2. Effects of Intermittent Seepage Flows

The models discussed so far are based on the assumption that seepage process is steady and continuous. However, seepage occurs only during periods immediately after episodes of precipitation in arid and semiarid zones. If the time intervals between episodes of precipitation is not large cumulative effects of individual seepage events can be considered as nearly equivalent to that of steady flow. This seems to be the case of the municipality of Jenipapo de Minas where meteorological records reveal a near regular pattern of rainy seasons. However, in cases where rains are sparse and irregular it is necessary to consider decay of thermal perturbations during periods when seepage is absent. This is a complex heat transfer problem for which analytical solutions are not easily available. Nevertheless, a simplified approach is possible for cases where the decay of thermal perturbation can be considered as equivalent to that of a medium undergoing conductive cooling. In such cases, a qualitative understanding of cooling curves can be obtained by considering temperature distributions of perturbed and unperturbed states as limiting conditions. The transition from the depth value corresponding to the perturbed state (z_p) to that for the unperturbed state (z_u) as a function of time (t) can be described by a relation of the type:

$$z\,(t) = z_u + \frac{z_p - z_u}{1 + \eta\,\sqrt{t}} \tag{5}$$

where η is a suitable scaling factor. Note that in equation 5 the depth of isotherm under consideration $z(t)$ is equal to z_p at time t equals zero (which may be considered as the instant of time at the end of a seepage flow). Its value approaches z_u as time approaches t^* (considered as a large time interval between seepage flows). The square root term in the denominator of the second term on the right-hand side of equation 5 imply that the cooling between seepage flows incorporate dependence on inverse square root of time, a standard practice geothermal heat conduction [19; 24] The scaling factor η is related to the thermal diffusivity of the medium. Lack of suitable observational data has prevented us from carrying out a practical test of thermal effects of intermittent seepage flows, based on equation 5.

5. Discussion and Conclusions

Seepage processes occur mainly in regions where aerated zones are thick and static levels of groundwater deep. Hence subsurface thermal perturbations by seepage flow are likely to be significant in arid and semiarid zones. Nevertheless, analysis of temperature log data for boreholes in central Brazil indicate that thermal effects of seepage flow at shallow depths are widespread, occurring in many localities with thick soil cover. Two illustrative cases are provided in Figure 8, as examples of seepage effects identified in temperature logs of boreholes penetrating tropical soil layers. The sites are Laje de Muriae (located in the southern parts of the State of Minas Gerais) and Lagoa de Confusão (in the northern part of the State of Tocantins).

Reduced temperature profiles for these sites are illustrated respectively in the left and right panels of Figure 8. In these localities surface material may be considered as falling into groups classified as Oxisoil and Cambisoil. Their occurrences are often recognized in morphoclimatic domains, described as ‘Caatinga’ (semi-arid lowlands) and ‘Cerrado’ (flat tropical highlands with savannah type vegetation).

According to [25] the soil layers occurring in these localities are products of tropical weathering processes and are characterized by significant porosity and permeability.

It is clear that the presence of thermally anomalous zone at shallow depths induced by seepage of meteoric waters has led to overestimation of climate warming episode. In the present work a method has been presented that may be employed for correction of thermal perturbations by seepage flow at shallow depths, in tropical and subtropical regions. In addition, results of geoelectrical surveys are presented as a convenient method for mapping subsurface layers affected by seepage flows.

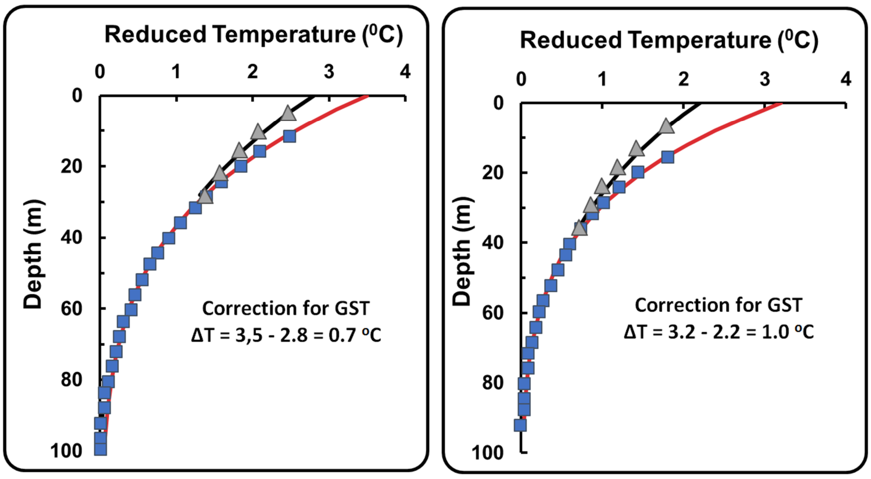

Figure 8. *Vertical distributions of reduced temperatures (square symbols) and values corrected for thermal perturbations by seepage flows (triangles). The continuous curves in red color are model fits that does not allow for seepage effects. The continuous curves in black color are model fits that incorporate corrections for seepage flows. The sites are in Southeast Brazil. The localities are Laje de Muriae (in the State of Minas Gerais) and Lagoa de Confusao (in the State of Tocantins). The sediment covers at these sites are Oxisoil and Cambisoil, respectively.*

The present work is focused on corrections in the procedure for extracting climate signals from thermal logs of shallow boreholes. In this context, note that a better understanding of climate signals at shallow depths is also of importance in procedures used for extracting signals of earlier climate episodes present at deeper depth levels [26; 27]. Lack of suitable observational data has prevented us from evaluating the thermal effects of intermittent seepage flows.

Acknowledgements

The authors acknowledge the Department of Geophysics of the National Observatory – ON/MCTIC, that provided financial support to carry out acquisition of field data. Thanks are also due to the Municipality of Jenipapo de Minas and the Group of Studies and Research in Geosciences and Engineering of the Jequitinhonha and Mucuri Valleys – GEOVALES, for providing operational support during field surveys.

References

[1] Cermak, V., (1971). Underground temperature and inferred climatic temperature of the past millennium, Palaeogrogr., Palaeoclimatol., Palaeoecol., 10, 1-19.

[2] Beck, A. E., 1977. Climatically perturbed temperature gradients and their effect on regional and continental heat flow means, Tectonophysics, 41, 17-39.

[3] Hamza, V. M., 1982, Research on measurement of subsurface temperatures: Importance in hydrogeology (in Portuguese). Revista de Águas Subterrâneas, v.5, 65-99.

[4] Lachenbruch, A. H., Sass, J. H. and Marshall, B. V., (1986). Changing Climate: Geothermal Evidence from Permafrost in the Alaskan Artic, Science, 234, 689-696.

[5] Lachenbruch, A. H., Claudouhos, T. T. and Saltus, R. W., (1988). Permafrost temperature and the changing climate, Proc. Fifth International Conference on Permafrost, Trondheim, Norway, 1-9.

[6] Shen, P. Y. and Beck, A. E., (1992). Palaeoclimate and heat flow density inferred from temperature data in the Superior Province of the Canadian Shield. Global and Planetary Change, 98, 143-165.

[7] Shen, P. Y. Wang, K., Beltrami, H. and Mareschal, J.-C., (1992). A comparative study of inverse methods for estimating climatic history from borehole temperature data, Palaeogeography, Palaeoclimatology, Palaeoecology, 98, 113-127.

[8] Hamza, V. M., Silva Dias, F. J. S., Gomes, A. J. L. and Terceros, Z. G. D., 2005. Numerical and Functional Representations of Regional Heat Flow in South America, PEPI, 152, 4, 223-256.

[9] Vieira, F. P., Gomes, J. L. S., Hamza, V. M. 2016. Studies of shallow geothermal field at Janipapo de Minas: Implications for selection of sites for underground dams in the region designated as “arid zone polygon” (in Portuguese). In: Proceedings VII Brazilian Geophysics Symposium - SBGf.

[10] Gomes, J. L. S., Vieira, F. P., Hamza, V. M., 2017. Use of geophysical surveys in selection of sites for underground dams in the municipality of Jenipapo. In: Proceedings of International Congress of the Brazilian Geophysical Society - SBGf. Rio de Janeiro.

[11] CODEMIG – Company for economic development of the State of Minas Gerais, 2012. Geologic map of the sheet Jenipapo, Brazil (in Portuguese). Sheet SE.23-X-D-III. http://www.portalgeologia.com.br/wp-content/uploads/2013/09/jenipapo.jpg (Accessed 01 February 2016).

[12] CPRM – Company for Exploration of Mineral Resources, 2005. Diagnostics of the municipality of Jenipapo de Minas. Project for catalogue for supply of groundwater, Valley of Jequitinhonha (in Portuguese). http://rigeo.cprm.gov.br/xmlui/bitstream/ handle/doc/16275/ rel_cadastro_aguas_sub_jenipapo_minas.pdf (Accessed 01 September 2015).

[13] Coggon, J. H., 1971. Electromagnetic and electrical modeling by the finite element method. Geophysics, 36, 132-155.

[14] Rijo, L., 1977. Modelling of electric and electromagnetic data, Ph. D. Thesis, University of Utah.

[15] Dey, A., Morrison, H. F., 1979. Resistivity modelling for arbitrarily shaped two - dimensional structures. Geophysical Prospecting, 27, 106-136.

[16] Loke, M. H., Acworth, I., Dahlin, T., 2003. A comparison of smooth and blocky inversion methods in 2D electrical imaging surveys. Exploration Geophysics, 34, 182-187.

[17] Birch, F.: The effects of Pleistocene climatic variations upon geothermal gradients, Am. J. Sci., 246, 729-760, 1948.

[18] Vasseur, G., Bernard, Ph., van de Mentebrouch, J., Kast, Y. and Jolivet, J., (1983). Holocene paleotemperatures deduced from geothermal measurements, Paleogeography, Paleoclimatology, Paleontology, 43, 237-259.

[19] Carslaw, H. S. and Jaeger, J. C., (1959). Conduction of Heat in Solids, 386pp, Oxford University Press, New York.

[20] Chisholm, T. J. and Chapman, D. S., (1992). Climate change inferred from analysis of borehole temperatures: an example from western Utah. J. Geophys. Res., 97, 14155-14175.

[21] Golovanova, I. V., Harris, R. N., Selezniova, G. V. and Stulc, P., 2001. Evidence of climate warming in the southern Urals region derived from borehole temperatures and meteorological data, Global and Planetary Change, 29, 167-188.

[22] Roy, S., Harris, R. N., Rao, R. U. M. and Chapman, D. S., (2002). Climate change in India inferred from geothermal observations, J. Geophys. Res., 107, B7, 5, 1-16.

[23] Bredehoeft, J. D.; Papadopulos, I. S. 1965. Rates of vertical groundwater movement estimated from the earth's thermal profile. Water Resour. Res. 1, 325-323.

[24] Hamza, V. M., Cardoso, R. R., Alexandrino, C. H., 2010, A Magma Accretion Model for the Formation of Oceanic Lithosphere: Implications for Global Heat Loss. International Journal of Geophysics, 2010, Article ID 146496, 16 pages, doi: 10.1155/2010/146496.

[25] Guimaraes, S. N. P., Hamza, V. M. and Silva, J. J., 2013. Airborne geophysical surveys in the north-central region of Goias (Brazil): Implications for radiometric characterization of tropical soils. Journal of Environmental Radioactivity, 116, 10-18.

[26] Hamza, V. M., Cavalcanti, A. S. B. and Benyosef, L. C. C., 2006, Surface thermal perturbations of the recent past at low latitudes –inferences based on borehole temperature data from Eastern Brazil. Clim. Past, 3, 513-526, 2007.

[27] Hamza, V. M. e Vieira, F. P., 2010, Climate changes of the recent past in the South American continent: Inferences based on analysis of borehole temperature profiles. In Climate Change – Geophysical Foundations and Ecological Effects, Edited by Juan Blanco and Houshang Kheradmand, Chapter 6, p. 113-136.